Inverse determination of material properties of timber beams reinforced with CFRP using the classical beam theory

K. SAAD ▪ Budapest University of Technology and Economics, Hungary
Budapest University of Technology and Economics, Hungary
A. LENGYEL ▪ Budapest University of Technology and Economics, Hungary
▪ lengyel.andras@emk.bme.hu

Érkezett: 2021. 09. 24. ▪ Received: 24. 09. 2021. ▪ https://doi.org/10.14382/epitoanyag-jsbcm.2022.6

Abstract

Fibre-reinforced polymers (FRP) are widely used to enhance the performance of structural elements of various materials, including timber. Measurements of reinforced beams mostly involve load-deflection relationships in order to experimentally verify mechanical improvements, while numerical simulations require material parameters for constitutive laws. In this study, a numerical method based on the classical beam theory is presented to inversely determine the elastic-plastic parameters of the timber material and the reinforcing FRP fabric using measurement data on full-scale composite beams. Data on bending tests of spruce beams obtained in a previous research stage are used to demonstrate the method. The method can provide material parameters for the full size composite structural element prepared under conditions relevant to actual design conditions, including the reinforcement preparation. It is found that the bilinear model is an adequate description for wood, and good agreement between simulated and measured data is obtained. Model material parameters are computed and presented for several specimens individually.

Keywords: spruce, beam, CFRP, modulus of elasticity, yield stress, bilinear model.
Kulcsszavak: lucfenyő, gerenda, CFRP, rugalmassági modulusz, folyási feszültség, bilineáris modell

Khaled SAAD
Has a MSc degree in Civil Engineering at Budapest University of Technology and Economics. He is a PhD student at the Department of Structural Mechanics under the supervision of András Lengyel working on strengthening timber beams with fibre reinforced polymers.

András LENGYEL
Is an associate professor at the Department of Structural Mechanics, Budapest University of Technology and Economics. He has PhD degree in Engineering at the University of Oxford. He has co-authored 39 journal and conference papers.

1. Introduction

Wood is considered one of the widely used materials in construction, especially for lightweight structures, due to its easy processing, outstanding physical and mechanical properties compared to its low density and appearance. Wood has a more complex mechanical behaviour than steel or concrete, and the analytical methods to describe its behaviour are more cumbersome due to its orthotropic natural behaviour. The potential increase of loads such as dead loads during service life and the ageing of timber may lead to the decommissioning of pre-existing timber structures, though often structural elements can be efficiently repaired or strengthened as an alternative.

Fibre-reinforced polymers (FRP) are composites formed by embedding high-strength fibres (usually glass or carbon) in an adhesive matrix (usually epoxy). Carbon fibre reinforced polymers (CFRP), due to their high stiffness and strength-to-weight ratio, have become easily applicable ways of strengthening structural materials, including wood, to enhance structural performance in several ways. Studies on reinforcement of timber aim to examine the improvement of flexural capacity, stiffness, and ductility of the structural elements experimentally, analytically or numerically. Results on various wood species, reinforcement types, and applications can be found in the literature. With no intention to give here a detailed, comprehensive review, it is noted that the increase in load-bearing capacity is typically in the range of approximately 20% to 50% and sometimes higher, see, e.g. in [1-4], while the increase in stiffness does not mostly exceed 30% or often is insignificant, and sometimes higher, see, e.g. in [1, 4, 5, 6]. Also, the ductility of the reinforced beams is in most cases enhanced see, e.g. [3, 7]. Thus it has been proven that application of FRP to timber is a viable reinforcement way; hence, efforts in analytical and numerical modelling are due.

The reinforcing elements take various shapes and sizes. Usually, they are sheets, strips, or rods parallel to timber grains inserted in the tensile zone of the timber to boost tension capacity but can also be applied for compression or wrapped around the beam. The thinnest typical single plies are approx. 0.165 mm thick or sometimes thinner (used, e.g. in [8-9]) but lamellae of various thicknesses in the range of a few millimetres were investigated by several researchers (e.g. [5, 10-13]), including, e.g. more than 2 mm thick bidirectional fabrics used in [6]. Rods and pultruded elements can take even larger dimensions. Reinforcement in the nanoscale by, e.g. CNTs (carbon nanotube) is also a possible field to investigate, see, e.g. [14].

Anisotropy of wood is somewhat similar to the transversely isotropic fibre-matrix composite material because of its stress-strain characteristics, failure modes, and predominant fibre direction, though it is more complex. Fortunately, the linear orthotropic material model with nine material constants can always be applied to describe the behaviour of timber in the elastic range. A number of previous studies have addressed the

analysis of the complex behaviour of carbon-reinforced timber beams by developing linear and non-linear mechanical models relying on experimental works and the finite element method (FEM), which provides a powerful numerical approach [11, 13, 15-19].

Numerical analysis requires constitutive models populated with appropriate material parameters. Fibre-reinforced composites are usually regarded as linearly elastic with brittle rupture, whereas a more sophisticated description is necessary for timber. Unfortunately, the linear orthotropic model is applicable only in the linear range, and non-linear stress-strain relationships are needed beyond that, especially in the compression range where several different variations have been used, e.g. perfectly plastic (e.g. [2, 11-12]), bilinear (e.g. [1, 20-22]), higher-order (e.g. [23]), etc. A tri-linear stress-strain diagram was proposed by [24] to analyse the failure behaviour of wood in the compression parallel to the grain. Furthermore, the bilinear anisotropic stress-strain relationship proposed by Hill can be applied to predict the orthotropic linear elastic–quasi rigid behaviour in tension as well as the orthotropic linear elastic–perfectly plastic and sometimes bilinear behaviour in compression satisfying the consistency conditions [24-25]:

$$\frac{\partial f}{\partial \sigma_{ij}} d\sigma_{ij} = 0 \qquad (1)$$

An orthotropic elastic and ideally plastic model was presented in [2] for the behaviour of timber beams strengthened with CFRP.

Material constants required for the numerical analysis are mostly obtained from the manufacturer, own experiments, or literature data. In the case of FRP, parameters of either the fibres or the prefabricated fibre–matrix composites are provided by the manufacturer. In the case of wood material, however, properties show a large variation depending on various factors, e.g. species, age, moisture content, density, location, etc. Properties may even differ from sample to sample and quite often are indicative only.

In an experimental study preceding the present work [4], four-point bending tests were performed on Norway spruce beams reinforced with CFRP fabric. Such experiments highlight various difficulties of acquiring adequate material data for the numerical analysis of these composite structures. Test specimens for measurement of material properties following standards may differ in quality from those under investigation, especially if old historical structures are to be reinforced. On the one hand, standardized testing of wood for compression parallel to grain has small scale specimens of prescribed length to width ratio producing a typical loading mechanism with splitting parallel with grains and partial lateral buckling. Also, the measured stress-strain curve may show significant variations with respect to the observed failure mode.

On the other hand, compression in full-scale timber beams under bending have different geometric conditions as the compression zone is not a stand-alone specimen. The elastic limit in compression and the non-linear behaviour of the material are important factors in the global behaviour in bending. The quality of FRP reinforcement is also a function of various factors. While factory produced lamellae are likely to follow the nominal specifications, manual in situ fabrication is prone to produce errors. As mentioned above, the stiffness increase due to reinforcing is generally moderate. It is often in good accordance with analytical predictions (see, e.g. [1, 10, 12, 13, 26-27]); however, several studies report experimental behaviour that differs from expectation to a lesser or larger degree and have to be considered as ill-performance (see, e.g. [5-6, 21, 28]). (Analytical derivation of stiffness is based on the fundamental elastic formulation stress resultants in inhomogeneous cross-sections as stiffness is interpreted in the elastic range.) As we experienced a similar phenomenon in our experimental study [4] as well, the present research aims to address this problem, utilizing the obtained measurement data.

Considering the above-mentioned challenges regarding material data, it may be prudent to apply inverse calculation of material properties of timber–CFRP composite structures. Very few studies have addressed that, for example, elastoplastic material model parameters in the generalized anisotropic Hill potential model were calculated for two wood species for the purpose of finite element modelling in [29]. The stress-strain behaviour of the Hill model was assumed to be linear elastic-quasi rigid in tension, bilinear ductile in compression. Validation was done by comparison of FE simulation with statistics of a sample of experimental data on small scale specimens.

This research was further inspired by an industrial project communicated to the authors where old timber beams extracted from a historical industrial building were offered for FRP reinforcement and testing. Measurements on composite beams of original timber material can provide the design of reinforcement of the remaining structural elements with realistic and actual material properties for both constituents.

This paper presents a numerical method for the indirect determination of material properties of timber–CFRP composite beams based on measured load-deflection curves. Measurement data obtained from own testing of full-size beams are used to illustrate the applicability of the method. It can address several difficulties in obtaining relevant material parameters as the composite is analysed in its entirety on a full scale as opposed to its constituents individually on a small scale, each specimen is investigated individually and not the whole sample statistically, various constitutive models can be implemented and recommendations given, and the FRP reinforcement is produced under the same conditions as expected in a real application. The outline of the paper is as follows: Section 2 briefly introduces the experiments, Section 3 elaborates the method, Section 4 presents the results through a selection of specimens, and the conclusions are summarized in Section 5.

2. Experiments

In a previous research project [4], a series of measurements were conducted on timber beams fitted with CFRP material to investigate the efficacy of reinforcing. The experimental program was designed to imitate the conditions corresponding to the manufacturer's intention. The aim was to test a technique that was not time-consuming and could be executed under

various conditions, including retrospective reinforcement on site. Accordingly, the fibre material provided by the manufacturer was a relatively thick fabric of pure carbon fibres (with no epoxy) in rolls. It was bidirectional with only 1 per cent in weft and 99 per cent in warp, the thickness is 1.4 mm when compact, and a volume ratio of ninety per cent was assumed. The epoxy resin was suitable for spreading with a roller.

A total of 44 beam specimens were prepared for four-point bending, see *Fig. 1.* The timber was sawn wood of Norway spruce (*Picea abies*). Eight specimens were left unaltered for reference, and the rest were reinforced with various amounts of fabric on the tension side. Twenty specimens were fitted with a single layer (1.4 mm thick), eight with a double layer (total 2.8 mm thick), and another eight with a narrow single layer (half-width of the beam). The four groups are also shown in *Fig. 1.*

The reinforcement was prepared in situ by spreading a thin layer of epoxy by a roller on the surface, then placing the fabric, and finishing with rolling a sufficient amount of epoxy to saturate the fabric and thus make the bond to the timber and form the composite simultaneously.

During the process, the magnitude of the load and mid-point displacement were measured and recorded digitally. These load-deflection curves provide the basis for the analysis introduced in the next section, though the method is not specific to these data.

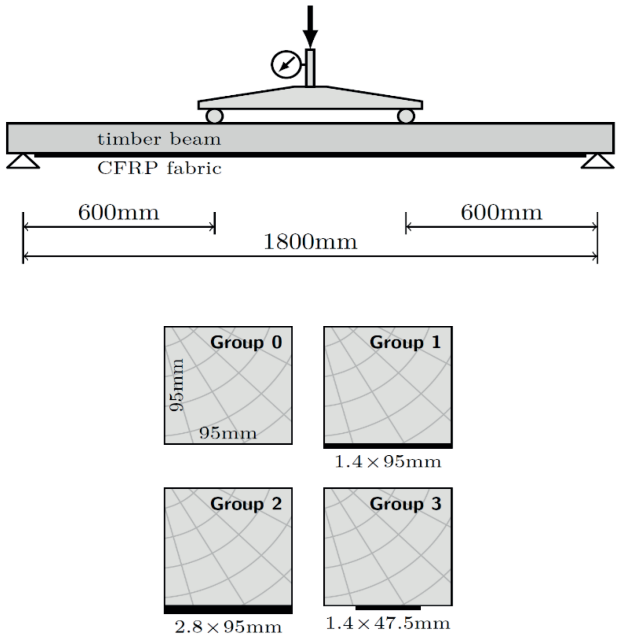

Fig. 1 Sketch of test arrangement and cross-sections with various reinforcement types.
1. ábra Kísérleti elrendezés vázlata és a keresztmetszet különböző megerősítésekkel.

3. Material constants

The reinforced beam is a three-dimensional continuum composed of an orthotropic wooden part and a transversely isotropic fibre-matrix composite such that the fibre/grain direction of both materials is aligned with the axis of the beam. Since significant stresses and strains are not expected in the transverse direction, the classical Euler beam theory is applied here, assuming rigid cross-sections and no shearing deformations. Therefore, the constitutive equations need to be given in the axial direction only.

The CFRP composite is linearly elastic for tension with brittle rupture at the end of its strength. The fabric is attached to the tension side of the beam (lower chord), and thus compressive stresses do not occur. The reinforcement is then given by the modulus of elasticity E_r as the only material parameter.

The wood is linearly elastic in a limited initial phase of the loading, then some kind of nonlinearity is usually considered. In the compression zone, the wood is often modelled as linearly elastic and perfectly plastic, bilinear (with hardening or softening), or some kind of higher-order relationship between stresses and strains beyond the elastic limit. In the tension zone, it is customary to consider brittle rupture, though other models can also be defined (e.g. bilinear).

The constitutive equation is formulated for the reinforcement as $\sigma_r = p_0\varepsilon_r$, where σ_r and ε_r are the stress and strain in the reinforcement, respectively, and parameter p_0 represents modulus of elasticity E_r. For the wood material, we have $\sigma_w = \sigma_w(\varepsilon_w; p_1, \ldots, p_n)$, where σ_w and ε_w are the stress and strain in the wood, respectively, and p_i $(i = 1, \ldots, n)$ are the material parameters associated with the chosen model.

Deformations in the Euler beam theory are characterized by the curvature κ. In terms of the material parameters, strains and then stresses can be formulated for any given κ, see *Fig. 2.* The shape of the stress diagram depends on the stress-strain curve of the chosen model. In this study, it is assumed that reinforcement is applied in an unloaded state of the beam. If initial loading is considered, the pre-existing stress and strain states need to be incorporated in the models [30].

The stress resultant in the cross-section provides the bending moment M associated with curvature κ. This way, the M - κ diagram can be generated for a selected interval of the curvature. For any given load F, the bending moment diagram and, therefore, the curvature diagram of a beam with given dimensions and loading arrangement can be determined, e.g. for the beam shown in *Fig. 1.* Finally, the mid-span deflection is easily obtained using geometric relationships based on the principle of small displacements.

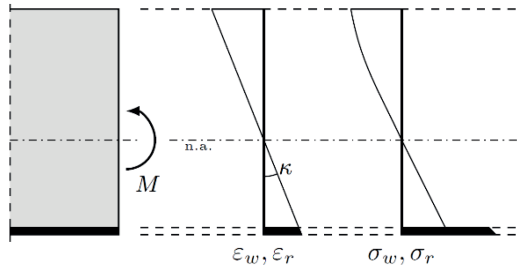

Fig. 2 Axial stresses and strains in the Euler beam.
2. ábra Normálfeszültségek és -alakváltozások az Euler-gerendában.

For a selected set of load values F_j $(j = 1, \ldots, m)$ numerically simulated mid-span deflections $d^{\text{sim}}(p_i)$ can be generated. Naturally, the load values need to be chosen to match the range of the load data recorded during the measurement. Measured mid-span deflections (d_j) associated with the loads are to be

compared with the above mentioned simulated values. The basis for the comparison is an error function we define as

$$f_{err}(p_i) = \int_0^{F_{max}} \left[d - d^{sim}(p_i) \right]^2 dF \quad (2)$$

which is a non-negative quantity. For computational purposes, the integral is replaced with a discretized form of function (1) based on the trapezoidal rule as:

$$f_{err}(p_i) = \sum_{j=1}^{m-1} \frac{1}{2} \Delta F_j (g_j + g_{j+1}) \quad (3)$$

Where $g_j = (d_j - d_j^{sim}(pi))^2$ and $\Delta F_j = F_{j+1} - F_j$. The sampling of load values ought to be dense enough to represent the measured data accurately while keeping the computational costs acceptable. The adequacy of any set of parameters p_i, (i = 0, . . . , n) is then characterized by the magnitude of the error obtained by Eq. (2). The objective is to find the optimal set of parameters p_i, which minimizes $f_{err}(p_i)$ for a given load-deflection data set (F_j, d_j). The error function cannot be expressed explicitly as it requires lengthy numerical computations; therefore, a gradient approach is not convenient. Since it is known that an optimum of the objective function may not be found starting from an arbitrary configuration [31], and the measured data are irregular to some extent, it is assumed that several local minima may exist. Therefore, a robust grid search is applied in the parameter space to find a first approximation of the optimal parameters (grid search or parameter sweep is a numerical strategy for nonlinear inverse problems and can be competitive for a small number of parameters. It examines trial values in a regular grid in the parameter space and chooses the one with the smallest error. See, e.g. Menke, 2012., Sec. 9.4. [32]). Then the grid is refined in a few consecutive steps until the required precision is achieved, which is set to 1 N/mm² for moduli of elasticity and 10^{-3} N/mm² for stresses (e.g. compression yield stress).

4. Results

The method is demonstrated by the load-deflection curves obtained in the tests introduced in Section 2. The four specimen groups are shown separately in *Fig. 3.* The mean values of ultimate load and elastic stiffness in the initial linear range of the curves are summarized in *Table 1.* (Stiffness was determined by fitting a regression line for the range between 10% and 40% of the ultimate load for each specimen, obtaining coefficient of determination (R^2) of 99.2% and above.) For a detailed statistical analysis and evaluation of the measurements, see [4].

4.1 Wood models

Four material models are chosen for the wood, see *Fig. 4.* In the first case, nonlinearity is accounted for by plasticity in the compression zone. Wood is considered perfectly plastic for compression beyond the elastic limit, while unlimited tension capacity is assumed. This model is characterized by two parameters, modulus E_w and plastic yield stress σ_{cy}. The tensile strength of the wood corresponds to the endpoint of the load-deflection curves.

Spec. group	Number of specimens	Stiffness [kN/mm]	Ultimate load [kN]
0	8	0.6477	23.220
1	20	0.7463	30.527
2	8	0.7534	30.959
3	8	0.7068	27.448

Table 1 Mean values of elastic stiffness and ultimate load in specimen groups.
1. táblázat A rugalmassági modulusz és a törőteher átlagértékei a tesztcsoportokban

In the second case, a brittle rupture in tension is considered, while plasticity in compression is omitted to investigate the effect of tensile failure only. It implies that no additional load-bearing capacity is available after the first rupture. This model is characterized by the modulus E_w and the ultimate tensile stress σ_{tu}. This approach can be used if rapid progressive collapse is assumed following the first rupture. In the presence of reinforcement (groups 1 to 3), however, further load-bearing is possible.

The third case combines the first and the second (three parameters: E_w, σ_{cy}, and σ_{tu}), i.e. nonlinearity in both tension and compression.

The last case assumes bilinear behaviour in the compression zone and unlimited tension capacity. The parameters are E_w, σ_{cy}, and E_t, the latter one referring to the tangent modulus in compression. This way, the compression behaviour is refined by allowing hardening or softening after the elastic limit. With the tangent modulus, the load-deflection curve can be followed more closely. Tension rupture is not considered in this case. In all cases, modulus E_r for the reinforcement is also added to the parameter set for groups 1 to 3 (but not for group 0). A few out of the 44 specimens had insignificant non-linear behaviour, where only the elastic moduli had to be determined. In the majority, however, some kind of nonlinearity is observed; therefore, Models 1 to 4 in *Fig. 4* are applied to the timber.

4.2 Examples

A detailed analysis is not possible to be presented here for all specimens, but the method can be well illustrated in detail through a selected few. First, load-deflection curves of a non-reinforced specimen are shown in *Fig. 5.* The measured data are plotted in dash-dotted lines while the rest are numerically simulated curves obtained by using models in *Fig. 4*, respectively. The first model considers linearly elastic and perfectly plastic behaviour in compression and unlimited tension capacity. The load-deflection curve obtained by the optimization method apparently follows the measured data quite closely both in the linear and the non-linear range. The second model considers tension rupture only. Since rupture involves immediate failure, no nonlinearity occurs, and the simulated line is inevitably straight and cannot approximate the measured data. The third model is the extension of the first with tension rupture. Since rupture can occur only at the final failure, the results are identical to those for the first model. However, the plots suggest that further improvement may be possible, so the fourth model is applied, which incorporates softening or hardening beyond the elastic limit in the compression range. With this model, a better approximation is achieved, as evident in *Fig. 5.* The

adequateness of each model is also represented by the error values (obtained using (2)) associated with the four models, i.e. 12866.20 Nmm^2, 432865.16 Nmm^2, 12866.20 Nmm^2, 747.10 Nmm^2, respectively. Optimal material parameters for the models are also shown in *Fig. 5*.

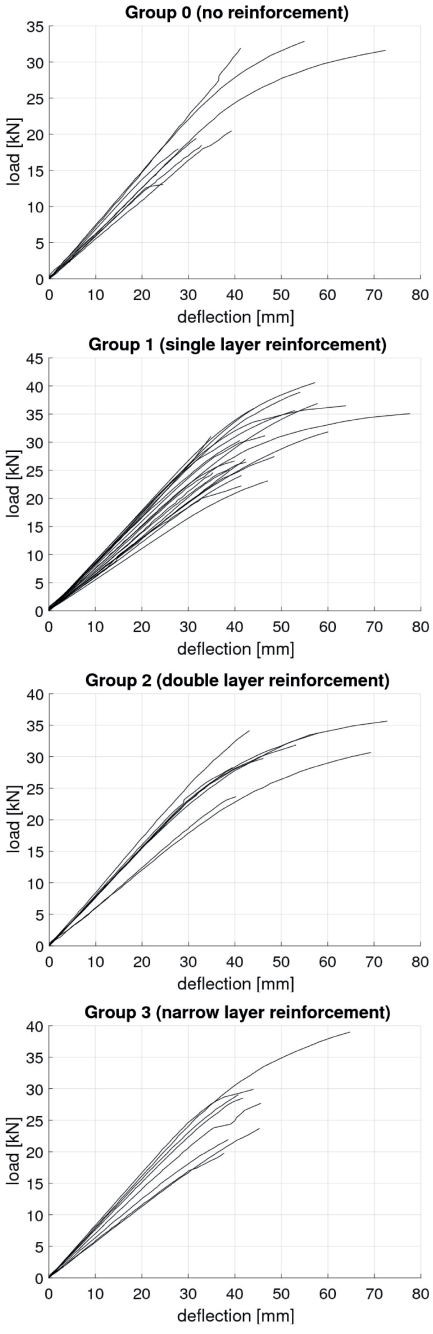

Fig. 3 Load-deflection curves for all specimen groups.
3. ábra Erő-lehajlás-görbék minden tesztcsoportban.

The second example is a specimen with a single layer reinforcement, see *Fig. 6*. In this case, extensive plastic behaviour is observed with a definite curvature in the plot. The first model captures the general trend of the measured data curve but clearly not adequately enough. The third model again gives the same result. The fourth model is again expected to yield a better approximation by introducing possible hardening or softening behaviour beyond the elastic limit in compression. It is found that with appropriate softening, the curvature of the non-linear part of the curve can be approximated more closely. The material properties are indicated in the figure. In the case of the second model, tension rupture does not involve the immediate failure of the structure since the fibre reinforcement can replace timber in tension. However, the sudden loss of load-bearing in timber results in a quick increase of displacement and hardening occurs only when the reinforcement develops sufficient stress. It results in a concave curve, which clearly does not follow the measured curve. Accordingly, the error values associated with the models are 27460.50 Nmm^2, 83269.50 Nmm^2, 27460.50 Nmm^2, 1373.87 Nmm^2, respectively. Comparison of models 1 and 4 clearly shows that the fourth model with bilinear behaviour can significantly improve the results, as seen in the figure.

The third example is a specimen with a double layer reinforcement, see *Fig. 7*. In this case, the findings are similar to those in the previous example. The error values associated with the models are 12404.40 Nmm^2, 78458.04 Nmm^2, 12404.40 Nmm^2, and 8882.93 Nmm^2, respectively. However, in this case, even the fourth model cannot approximate the measurements as well as before. The plot shows that the measured data curve is not smooth but has a breakpoint near the end (a localised change of slope), which suggests that a partial tensile failure might have taken place without causing total collapse. Model 2 with tension rupture can only give a highly exaggerated approximation with a sharp breakpoint. In order to capture the phenomenon of the delicate breakpoint in the curve, a more sophisticated material model is needed, which handles partial rupture within the cross-section. With appropriate parametrization, such a model can be formulated, though it is not the topic of this study.

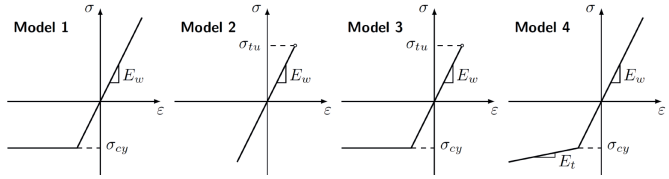

Fig. 4 Stress-strain curves for four different wood models.
4. ábra Feszültség-alakváltozás-görbék négy különböző faanyagmodellre.

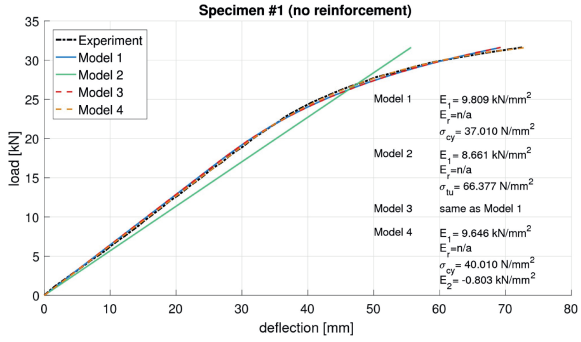

Fig. 5 Measured and simulated load-deflection curves for specimen 1.
5. ábra Mért és számított erő-lehajlás-görbék az 1. Mintadarabra.

The last example is a specimen with a single layer reinforcement. The load-deflection curve shows a moderate

nonlinearity, and the maximum deflection is average, thus representing a typical case *(Fig. 8)*. Though for this specimen, the difference between the individual models is visually not as accentuated as in the previous cases, the numeric computation can clearly evaluate and rank the models. The results are similar to those of the second example. The error values associated with the four models are 1093.10 Nmm^2, 3048.03 Nmm^2, 1093.10 Nmm^2, 641.97 Nmm^2, respectively. Here again, the fourth model provides the best approximation improving the outcome of the elastic-plastic model by introducing the bilinearity.

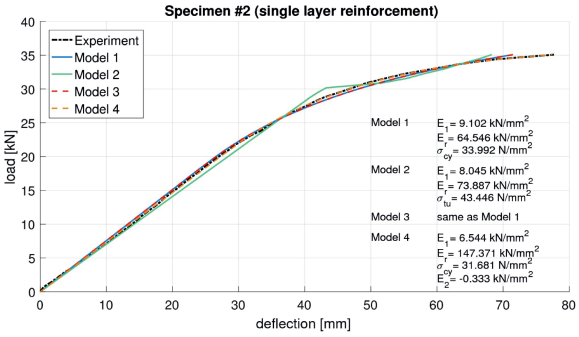

Fig. 6 Measured and simulated load-deflection curves for specimen 2.
6. ábra Mért és számított erő-lehajlás-görbék az 2. Mintadarabra.

4.3 Comparison of models

The selected specimens shown in the previous subsection provide a good sample of the general behaviour. *Table 2* summarizes the statistics of the results for all models. Numbers in the table are the mean values of the parameters in each group, with corresponding standard deviations shown in parentheses. Reinforcement modulus is not applicable for group 0 (n/a).

The basic model with perfect plasticity in compression can generally capture the trend of the load-deflection curves in most cases, except when the specimen shows insignificant nonlinearity (brittle rupture before plasticity could take place) or when a localized change occurs, which breaks the smooth character of the curve (e.g. partial rupture at a particular point during the loading process, etc.). The average modulus of elasticity of the wood material is between 8.16 kN/mm^2 and 9.89 kN/mm^2 in the four specimen groups, with a relative standard deviation between 11.5% and 18.8%. These values are within the typical range for these species. Average compression yield stresses range between 32.228 N/mm^2 and 36.59 N/mm^2 with a relative standard deviation between 15.3% and 19.7%. Note that similar results were obtained in the four specimen groups, which indicates that the method can adequately extract wood material properties from the data regardless of the amount of reinforcement. Results on the reinforcement are somewhat unexpected. In groups 1 to 3, the average moduli range between cca. 45 kN/mm^2 and 85 kN/mm^2 with large relative standard deviations (20 kN/mm^2 to 50 kN/mm^2).

The second model, which considers only tension rupture, gives incorrect results, as apparent through the examples shown in the previous subsection. It is found through the simulations that rupture in the tension zone at the full width of the cross-section results in such a large immediate loss of load-bearing capacity that the slope of the load-deflection curve drops significantly. None of the test specimens exhibited such extreme behaviour, except at the final failure just prior to collapse. Therefore, tensile rupture alone cannot be responsible for the nonlinearity of the structure, and the results of Model 2 are discarded. As seen through the example specimens in the previous section, Model 3, which combines plastic compression with tension rupture, gives results similar to Model 1 since

Mod	Gr	E_w(kN/mm^2)	E_r(kN/mm^2)	δ_{cy}(N/mm^2)	δ_{tu}(N/mm^2)	E_t(kN/mm^2)
1	0	9.899 (1.142)	n/a (n/a)	32.228 (6.340)		
	1	8.578 (1.343)	77.139 (28.850)	36.594 (5.589)		
	2	8.168 (1.534)	45.813 (24.268)	34.067 (5.567)		
	3	9.129 (1.252)	85.395 (51.275)	34.717 (5.356)		
2	0	9.603 (1.120)	n/a (n/a)		48.748 (16.158)	
	1	7.780 (1.074)	100.903 (42.405)		35.374 (10.346)	
	2	7.562 (0.646)	52.646 (20.486)		31.940 (5.629)	
	3	8.896 (1.215)	77.860 (44.843)		49.032 (7.582)	
3	0	9.899 (1.142)	n/a (n/a)	32.228 (6.340)	53.883 (21.450)	
	1	8.561 (1.357)	77.445 (30.999)	36.723 (5.628)	54.784 (14.371)	
	2	8.168 (1.534)	45.813 (24.268)	34.067 (5.567)	46.352 (12.218)	
	3	9.129 (1.252)	85.395 (51.275)	34.717 (5.356)	50.697 (9.707)	
4	0	9.892 (1.127)	n/a (n/a)	31.307 (8.356)		0.266 (3.838)
	1	8.685 (1.757)	74.728 (41.563)	37.177 (7.106)		-0.557 (2.282)
	2	8.448 (1.466)	40.216 (19.546)	35.270 (3.248)		-0.844 (2.191)
	3	9.547 (1.438)	62.577 (31.414)	34.538 (7.693)		0.614 (2.284)

Table 2 Mean values and standard deviations of optimal material parameters (wood modulus E_1, reinforcement modulus E_r, wood compression yield stress σ_{cy}, wood tension ultimate stress σ_{tu}, wood tangent modulus E_t) in all specimen groups (Gr) for all models (Mod). Standard deviations are given in parentheses. Ultimate stresses shown in italics are computed at failure load.
2. táblázat Optimális anyagi paraméterek átlaga és szórása (E_1: fa rugalmassági modulusza, E_r: megerősítés rugalmassági modulusza, σ_{cy}: fa folyási feszültsége nyomásra, σ_{tu}: fa húzószilárdsága, E_t: fa érintőmodulusza) minden tesztcsoportban (Gr) minden modellre (Mod). A szórások zárójelben vannak megadva. A dőlten szedett szilárdságértékek a törőteherre vonatkoznak.

the latter behaviour is not dominant. Nearly in all cases, the results are the same, i.e. for groups 0, 2, and 3, where the statistics give the same figures in terms of wood modulus and plastic yield stress. Ultimate tension stresses shown in the table are computed at the instant of failure and not obtained through the optimization algorithm; such figures are shown in italics. However, in the case of group 1 (with a single layer of reinforcement), some specimens differ, so the mean values for modulus and plastic yield stress are slightly different. Here the statistics refer to the results of the optimization, though the calculated failure stresses are similar, too.

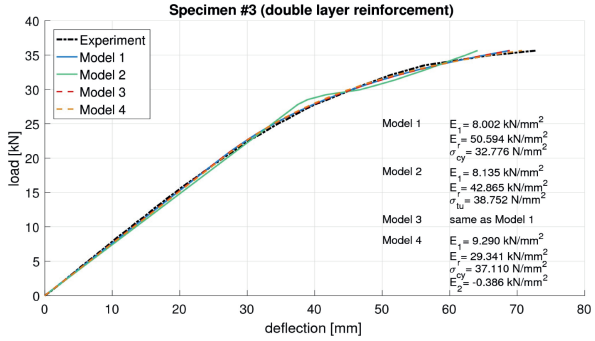

Fig. 7 Measured and simulated load-deflection curves for specimen 3
7. ábra Mért és számított erő-lehajlás-görbék az 3. Mintadarabra

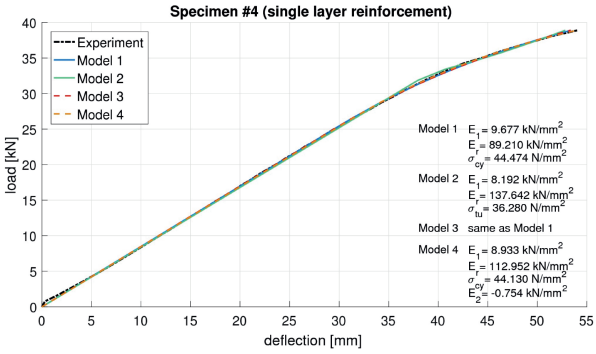

Fig. 8 Measured and simulated load-deflection curves for specimen 4.
8. ábra Mért és számított erő—lehajlás-görbék az 4. Mintadarabra.

Model 4 provides the best approximation of the load-deflection curves among the models applied in this study. The average modulus of elasticity of the wood material is between 8.44 kN/mm^2 and 9.89 kN/mm^2 in the four specimen groups with relative standard deviation between 11.3% and 20.2%, similar figures to those obtained for Model 3. Average compression yield stresses range between 31.30 N/mm^2 and 37.17 N/mm^2 with a relative standard deviation between 9.2% and 26.6%. Yield stresses again are similar to previous results. This model incorporates possible softening or hardening in the plastic range via the tangent modulus, the mean values of which ranging between -0.844 kN/mm^2 and +0.614 kN/mm^2 in the four groups. Note that the standard deviations are large, indicating that the non-linear behaviour of individual species might differ substantially. Results on the reinforcement are also similar to previous results, with mean values ranging between cca. 40 kN/mm^2 and 75 kN/mm^2 with large relative standard deviations.

4.4 Discussion

The wood material models applied to the four different specimen groups lead to important conclusions. Timber beams tested in the experiments were obtained from the same source and possessed similar properties, as well as the fibre reinforcement, were prepared with the same material using the same technique. Numerical calculations presented here have verified that values obtained for the elastic modulus of wood are in the range characteristic of this species with ordinary variation (i.e. standard deviation). No significant differences are observed between specimen groups with different amounts of reinforcement. Each of the four wood material models had practically identical results with the exception of Model 2, in which case the validity of the results is questionable, as discussed previously.

In terms of the compression yield stresses in Models 1, 3, and 4, the results show very good agreement both modelwise and groupwise. It indicates that the algorithm was able to capture the nonlinearity of wood material regardless of the amount of reinforcement. However, differences are observed with respect to the degree of nonlinearity. Models 1 and 3 could simulate the curvature of the load-deflection diagram by means of the perfectly plastic behaviour in the compression zone, though they could not provide further adjustment.

Model 4, on the contrary, was able to fine-tune the degree of nonlinearity of the curve by applying potential softening or hardening. A significantly better fit is achieved through this though it is found that the tangent moduli are somewhat scattered in a range covering both positive and negative values. It indicates that the individual specimens were different in their compression behaviour.

The apparent inadequacy of Model 2 suggests that tension rupture should be modelled in a more refined way. Some of the specimens showed that observable tension rupture occurred during the loading process without causing complete failure, indicating that grains in the wood naturally have different strengths. Therefore, rupture may occur locally and gradually. In order to capture this effect, wood models that attribute different properties to different parts of the cross-section should be applied. With appropriate parametrization, the algorithm can incorporate such models. However, most specimens failed due to rupture in the tension zone immediately followed by progressive failure of the entire beam, indicating the importance of weak points in the timber material on the behaviour. The reliability of the specimens is primarily affected by the amount of material weak points such as defects or knots, see, e.g. [33]. Since wood is a natural material, this variation is reflected in the measured ultimate capacity of the specimens. Early tensile failure prevents the full utilization of the compression capacity of timber; therefore, the ductility of the beams varies in a range depending on when the rupture took place. An important difference between unreinforced and reinforced beams is manifested in the increased ductility of the latter case because the presence of reinforcement reduces the tensile stresses in the wood at the same load level, consequently higher ultimate load can be achieved, which in turn implies that the plastic compression capacity of the wood is utilized to a higher degree before failure.

In all groups with reinforcement, it has been observed that the modulus of the reinforcement material is below the theoretical modulus of the carbon fibre (i.e. 234 kN/mm^2 provided by the manufacturer). The reasons lie in the preparation of the CFRP fabric. The lamellae were prepared in situ by laying the glue on the surface with a roller forming the embedding matrix and the bond to the timber simultaneously. The procedure is efficient, can be applied for reinforcement in an arbitrary position, and provides an effective bond between fibres and timber. However, despite all its advantages, it has negative side effects. The extremely thin carbon fibres are sensitive to any action (e.g. bending) other than axial tension, so in situ preparation of the reinforcement lamellae inevitably inflicts damage to some degree. It is also inevitable to introduce geometric imperfections to the fibres (e.g. waviness), which further reduce the elastic modulus. Since the thickness of the fabric is larger than usual and the consistency of the epoxy is high, a considerable force is required to make the epoxy penetrate the fabric; hence its influence is large. The simulations have also shown that the elastic modulus is smaller in the case of double reinforcement because the application of the epoxy requires larger pressure and hence may cause a larger disturbance.

However, counter-intuitive, low increase in stiffness is by no means exceptional and has been reported in other research. Some researchers measured negligible increase simultaneously with considerable improvement of capacity. There are even recommendations not to consider fibre reinforcement for the purpose of enhancing stiffness see, e.g. [34]. Regarding the low increase in stiffness, see also other papers, e.g. [5, 10, 28]. Values of modulus of elasticity for the reinforcement obtained in this study are, in fact, in good agreement with the increase of stiffness obtained from the measurements. If the nominal modulus of the fibres as issued by the manufacturer are assumed (i.e. without any damage or imperfection), an increase of over 65% in stiffness is obtained by performing simple computations using the Euler beam model. A 3D finite element analysis gives the same figures. It obviously contradicts the observed 15 or 16% increase from the measurements (*Table 1*), however, if the values obtained from the algorithm are used, a good agreement with the measurements is achieved, providing verification for the results. A continuation of this research aims to model the behaviour of fibre reinforcement in detail.

5. Conclusions

In this study, a method was shown for the inverse determination of material properties of composite beams based on load-deflection diagrams using the Euler beam model. The optimal set of model constants minimizes the difference between the simulated and the measured load-deflection curves.

- The effectiveness of the method has been illustrated through a series of data obtained from four-point bending tests conducted in previous research on timber beams reinforced with CFRP fabric [4].
- Four different wood material models and one reinforcement model were applied, and the optimal material properties were computed. It is found that assuming linearly elastic behaviour in tension and bilinear stress-strain relationship in compression for the wood leads to a very accurate simulation of load-deflection curves.
- Material parameters of wood are realistic and in the typical range specific to the species in question. The effective modulus of the reinforcement falls short of the nominal value.

The advantages of the procedure presented here are that

- each specimen can be analysed individually;
- the obtained parameters may be considered more realistic with respect to the global behaviour of the beam if source data are obtained from tests on full-scale specimens (such as in this study) as opposed to data obtained from small scale ones;
- computation of parameters takes into consideration the real conditions and quality of the preparation of the reinforcement, enabling reinforcement design of existing structures with more reliable and appropriate data;
- computation of parameters also takes into consideration the actual conditions of timber that may not always be reproducible in a laboratory.

Note that constitutive models other than those presented here can also be implemented in the model, though the achieved accuracy does not demand that. The algorithm can also be used with other numerical solvers, e.g. with embedded user-created finite element analysis codes, or alternatively, coupled with commercially available finite element software. Test runs have already been performed.

As mentioned above, the computations have shown that the effective stiffness of the fibre material is reduced compared to the theoretical values. It is important to note that these results are in accordance with the measurements used in this study. The measured mean increase of stiffness due to reinforcement with respect to the unreinforced specimens is smaller than what one would theoretically obtain from the analysis of inhomogeneous elastic beams. It is by no means an exceptional case as a very low or moderate stiffness increase was reported in several works. As mentioned in the Introduction, in several cases, the results fall short of the expectations, though we have not found an appropriate discussion of the reasons behind. In the case of our study, we assume that the observed deficiency is due to geometrical imperfections and potential damage inflicted to the fibres by in situ preparation of reinforcement. Since the fabric was thicker than the typical ones, considerable pressure was required by rolling to make the epoxy saturate the fabric. The method presented here has also provided important data on the physical capabilities of the current preparation technique prompting to refine or adjust the treatment to exploit the full potential of fibre reinforcement. The future plans of the authors aim for detailed investigations along this line.

Acknowledgements

The presented work was conducted with the financial support of the K119440 project of the Hungarian National Research, Development and Innovation Office.

References

[1] A. Borri, M. Corradi, and A. Grazini. A method for flexural reinforcement of old wood beams with CFRP materials. *Composites Part B*, 36(2):143–153, 2005. doi = https://doi.org/10.1016/j.compositesb.2004.04.013

[2] T.P. Nowak, J. Jasieńko J, Czepiżak D. Experimental tests and numerical analysis of historic bent timber elements reinforced with CFRP strips. *Construction and Building Materials*, 40:197–206, 2013. doi = https://doi.org/10.1016/j.conbuildmat.2012.09.106

[3] Y.F. Li, Y.M. Xie, and M.J. Tsai. Enhancement of the flexural performance of retrofitted wood beams using CFRP composite sheets. *Construction and Building Materials*, 23(1):411–422, 2009. doi = https://doi.org/10.1016/j.conbuildmat.2007.11.005

[4] K. Andor, A. Lengyel, R. Polgár, T. Fodor, and Z. Karácsonyi. Experimental and statistical analysis of spruce timber beams reinforced with CFRP fabric. *Construction and Building Materials*, 99:200–207, 2015. doi = https://doi.org/10.1016/j.conbuildmat.2015.09.026

[5] A.M. de Jesus, J.M. Pinto, and J.J. Morais. Analysis of solid wood beams strengthened with CFRP laminates of distinct lengths. *Construction and Building Materials*, 35:817–828, 2012. doi = https://doi.org/10.1016/j.conbuildmat.2012.04.124

[6] T.W. Buell and H. Saadatmanesh. Strengthening timber bridge beams using carbon fiber. *Journal of Structural Engineering*, 131(1):173–187, 2005. doi = https://doi.org/10.1061/(asce)0733-9445(2005)131:1(173)

[7] Y.J. Kim, M. Hossain, and K.A. Harries. CFRP strengthening of timber beams recovered from a 32 year old quonset: Element and system level tests. *Engineering Structures*, 57:213–221, 2013. doi = https://doi.org/10.1016/j.engstruct.2013.09.028

[8] M. Corradi, A. Borri, L. Righetti, and E. Speranzini. Uncertainty analysis of FRP reinforced timber beams. *Composites: Part B*, 113:174–184, 2017. doi = https://doi.org/10.1016/j.compositesb.2017.01.030

[9] P. de la Rosa García, A.C. Escamilla, and M.N.G. García. Bending reinforcement of timber beams with composite carbon fiber and basalt fiber materials. *Composites Part B*, 55:528–536, 2013. doi = https://doi.org/10.1016/j.compositesb.2013.07.016

[10] J. Fiorelli and A.A. Dias. Analysis of the strength and stiffness of timber beams reinforced with carbon fiber and glass fiber. *Materials Research*, 6:193–202, 2003. doi = https://doi.org/10.1590/s1516-14392003000200014

[11] G.M. Raftery and A.M. Harte. Nonlinear numerical modelling of FRP reinforced glued laminated timber. *Composites Part B: Engineering*, 52:40–50, 2013. doi = https://doi.org/10.1016/j.compositesb.2013.03.038

[12] Y. Nadir, P. Nagarajan, M. Ameen, and M. Arif M. Flexural stiffness and strength enhancement of horizontally glued laminated wood beams with GFRP and CFRP composite sheets. *Construction and Building Materials*, 112:547–555, 2016. doi = https://doi.org/10.1016/j.conbuildmat.2016.02.133

[13] Y.J. Kim and K.A. Harries. Modeling of timber beams strengthened with various CFRP composites. *Engineering Structures*, 32(10):3225–3234, 2010. doi = https://doi.org/10.1016/j.engstruct.2010.06.011

[14] O¨. Civalek, S. Dastjerdi, and B. Akgo¨z. Buckling and free vibrations of CNT-reinforced cross-ply laminated composite plates. *Mechanics Based Design of Structures and Machines*, 2020. Published online 21 May 2020. doi = https://doi.org/10.1080/15397734.2020.1766494

[15] D.A. Tingley. *The stress-strain relationships in wood and fiber-reinforced plastic laminae of reinforced glue laminated wood beams*. Ph.D. thesis, Oregon State University, Corvallis, OR, 1996.

[16] C.P. Kirlin. *Experimental and finite-element analysis of stress distributions near the end of reinforce- ment in partially reinforced glulam*. Ph.D. thesis, Oregon State University, 1996. url = http://hdl.handle.net/1957/12262

[17] E. Serrano. Glued-in rods for timber structures - a 3D model and finite element parameter studies. *International Journal of Adhesion and Adhesives*, 21(2):115–127, 2001. doi = https://doi.org/10.1016/S0143-7496(00)00043-9

[18] B. Kasal and A. Heiduschke. Radial reinforcement of curved glue laminated wood beams with com- posite materials. *Forest Products Journal*, 54(1):74–79, 2004.

[19] M. Khelifa, N. Vila Loperena, L. Bleron, and A. Khennane. Analysis of CFRP-strengthened timber beams. *Journal of Adhesion Science and Technology*, 28(1):1–14, 2014. doi = https://doi.org/10.1080/01694243.2013.815096

[20] J. Fiorelli and A.A. Dias. Glulam beams reinforced with FRP externally-bonded: theoretical and ex- perimental evaluation. *Materials and Structures*, 44:1431–1440, 2011. doi = https://doi.org/10.1617/s11527-011-9708-y

[21] H. Johnsson, T. Blanksvärd, and A Carolin. Glulam members strengthened by carbon fibre reinforce- ment. *Materials and Structures*, 40:47–56, 2006. doi = https://doi.org/10.1617/s11527-006-9119-7

[22] K.-U. Schober, A.M. Harte, R. Kliger, R. Jockwer, Q. Xu, and J.-F. Chen. FRP reinforcement of timber structures. *Construction and Building Materials*, 97:106–118, 2015. doi = https://doi.org/10.1016/j.conbuildmat.2015.06.020

[23] Y.F. Li, M.J. Tsai, T.F. Wei, and W.C. Wang. A study on wood beams strengthened by FRP composite materials. *Construction and Building Materials*, 62:118–125, 2014. doi = https://doi.org/10.1016/j.conbuildmat.2014.03.036

[24] D.M. Moses and H.G. Prion. Anisotropic plasticity and failure prediction in wood composites. Re- search report, University of British Columbia, Canada, 2002. url = https://www.semanticscholar.org/paper/ANISOTROPIC-PLASTICITY-AND-FAILURE-PREDICTION-IN-Moses/7d3354bf340e9af1ab19a16702c8cb28015143b3

[25] ANSYS Inc. *ANSYS advanced analysis techniques guide*, 2007.

[26] G.M. Raftery and A.M. Harte. Low-grade glued laminated timber reinforced with FRP plate. *Compos- ites: Part B*, 42:724–735, 2011. doi = https://doi.org/10.1016/j.compositesb.2011.01.029

[27] J.R. Gilfillan, S.G. Gilbert, and G.R.H. Patrick. The use of FRP composites in enhancing the structural behavior of timber beams. *Journal of Reinforced Plastics and Composites*, 22:1373–1388, 2003. doi = https://doi.org/10.1177/073168403035583

[28] P. Neubauerová. Timber beams strengthened by carbon fiber reinforced lamellas. *Procedia Engineering*, 40:292–297, 2012. doi = https://doi.org/10.1016/j.proeng.2012.07.097

[29] J. Milch, J. Tippner, V. Sebera, and M. Brabec. Determination of the elasto-plastic material charac- teristics of norway spruce and european beech wood by experimental and numerical analyses. *Holz- forschung*, 70(11):1081–1092, 2016. doi = https://doi.org/10.1515/hf-2015-0267

[30] A. Garsteckl. Optimal redesign of elastic structures in the state of initial loading. *Journal of Structural Mechanics*, 12:279–301, 1984. doi = https://doi.org/10.1080/03601218408907473

[31] W. Prager. Unexpected results in structural optimization. *Journal of Structural Mechanics*, 9:71–90, 1981. doi = https://doi.org/10.1080/03601218108907377

[32] Menke, W., 2012. Geophysical data analysis: discrete inverse theory: MATLAB edition (Vol. 45). Academic press. url= https://books.google.hu/books?id=sUDAqFV_oRAC

[33] O. Ditlevsen. Reliability against defect generated fracture. *Journal of Structural Mechanics*, 9:115– 137, 1981. doi = https://doi.org/10.1080/03601218108907379

[34] H. Alhayek and D. Svecova. Flexural stiffness and strength of GFRP-reinforced timber beams. *Journal of Composites for Construction*, 16:245–252, 2012. doi = https://doi.org/10.1061/(asce)cc.1943-5614.0000261

Ref.:
Saad, K. – **Lengyel**, A.: *Inverse determination of material properties of timber beams reinforced with CFRP using the classical beam theory*
Építőanyag – Journal of Silicate Based and Composite Materials, Vol. 74, No. 1 (2022), 32–40. p.
https://doi.org/10.14382/epitoanyag-jsbcm.2022.6